

Twisted 3D holograms for self-referencing interferometers in metrology and imaging

Martin Berz¹ and Cordelia Berz¹

¹IFE Institut für Forschung und Entwicklung, 81675 Munich,
Trogerstr. 38, Germany, martin.berz@ife-project.com

(Dated: November 28, 2016)

The interference between radiation fields superposed appropriately contains all available information about the source. This will be recapitulated for coherent and incoherent fields. We will further analyze a new kind of twisted 3D interferometer which allows us to generate interferograms with high information content. The physical basis for these devices is the geometric parallel transport of electric fields along a 3D path in space. This concept enables us to build very compact 3D interferometers.

I. INTRODUCTION

In some cases, modern optical applications need an interference between a field and a rotated copy of this field. The rotational shearing interferometer[3] is an example for this. More general applications can be found in imaging and self-referencing interferometers (SRI) [4][5].

The following common methods are known to generate such a superposition. They are called 'component based rotations'.

- two lenses in a beam expander configuration, e.g. two lenses of focal length f in a distance $2f$, which actually flip the field by 180° using a Mach-Zehnder interferometer [4].
- two Dove prisms in both paths of a Mach-Zehnder interferometer [3].
- use of retro reflectors in a Michelson interferometer [3].

It is the purpose of this report to describe a new geometric method for the generation of such interferograms using parallel field transport.

II. PARALLEL TRANSPORT IN 2D AND 3D SPACE

Field rotations due to the parallel transport of an electric field along the light beam do not play a vital part in most optical systems. These systems are called 'flat'. One reason is that experimentally, the deviation from 'flatness' can only be determined if two different field transports are compared. This is normally an interferometric setup which has not been fully investigated yet.

The expression 'field transport' means that the field is transported along paths in 3D space. In a first, simple approach, the term 'parallel transport' can be understood as the 'best possible projection' of the electric field on the vector space orthogonal to the propagation direction of light. Such a projection is necessary to maintain the transversal wave character if the direction of light changes. More accurate definitions of the term 'parallel transport' can be given in differential geometry. Yet,

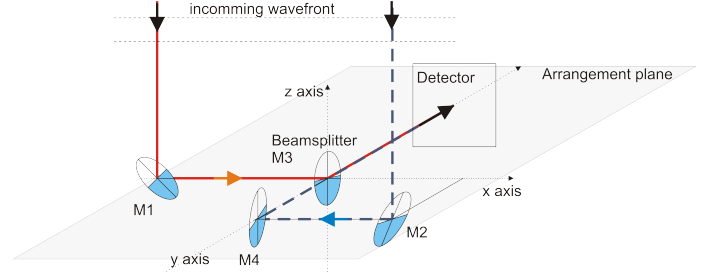


FIG. 1. One of the simplest 3D interferometer setups with field rotation. The interferometer uses a division of the wavefront, i.e. different parts of the incoming wave are fed to the device entries. The mirrors M1,M2,M4 and the beam splitter M3 are situated in the arrangement plane which is perpendicular to the incoming central beam. The central beam is defined by the property that the two beams have exactly the same direction after the superposing beamsplitter. The detector is perpendicular to the direction of the central beam. This implies that the central beam possesses no wave vector component in the detector plane.

this is not needed here since firstly a strict application of Maxwell's equations always leads to the correct result, and secondly we transport the electric fields by reflections on mirror like surfaces only. Thus, the mapping from the incoming to the outgoing field is straightforward.

However, the concept of parallel transport is helpful to understand the mechanism by which the Maxwell calculus leads to mutually rotated fields.

It immediately follows from the preceding introduction that such a parallel transport does not give a rotation if the field paths are purely in a 2D plane. In 2 dimensions, the rotation at the superposition point of two paths is independent of the specific path since rotations in 2D space commute. This behavior obviously changes if components are inserted into the 2D path that rotate the field. This is for instance used in a rotational shearing interferometer where Dove prisms are inserted into the path [3] (component based rotation). Outside the components, the central light path in the two branches is still contained in a 2D plane. Therefore, such an interferometer is called a 2D interferometer.

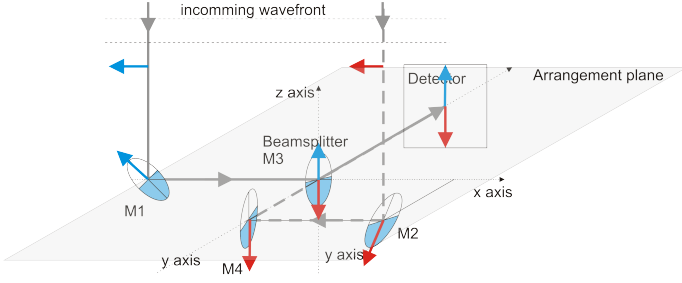


FIG. 2. The parallel transport of field directions 1 along branch 1 and 2. It can be seen that one direction at the device entrance is parallel transported to two opposite directions whereby the direction depends on the path.

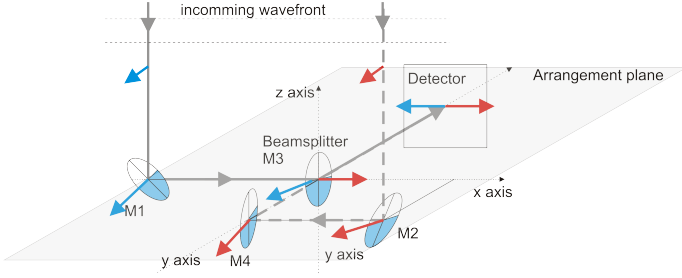


FIG. 3. The parallel transport of field directions 2 along branch 1 and 2. It can be seen that one direction at the device entrance is parallel transported to two opposite directions whereby the direction depends on the path.

In contrast, a 3D interferometer is characterized by the property that the central light paths do not lie in one and the same plane, not even approximately.

This definition of a 2D and a 3D interferometer is independent of the fact that all physical interferometers are actually built in a three dimensional space.

III. FIELD TRANSPORT IN A INTERFEROMETER: 3D VS. 2D

In this paper we will explore the field transport properties of a 3D interferometer.

Figure 1 shows the generic system for a 3D interferometer, the simplest system being a wavefront division interferometer. For any incoming plane wave this interferometer generates a superposition between a plane wave propagated by branch 1 and 2, respectively. For devices similar to the one shown in Figure 1 a central beam can be found that has the property that the \vec{k} vectors of the outgoing beams originating from branch 1 and 2 are exactly identical. Provided the path difference between branch 1 and 2 is within the coherence length, this leads to either constructive or destructive interference.

The beams in branch 1 and 2 have wave vectors called

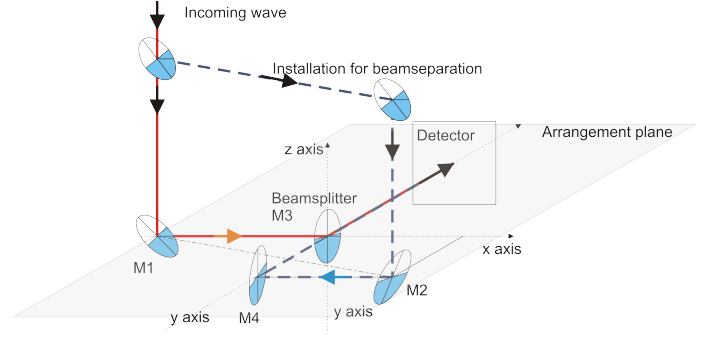


FIG. 4. The generic 3D interferometer of Figure 1 combined with an installation for beam separation. This yields an interferometer with 'amplitude division'. The beam separation is achieved by two reflections displacing one of the two beams. It does not introduce a rotation in the field transport. Thus, the field rotation properties of Figure 1 are unchanged.

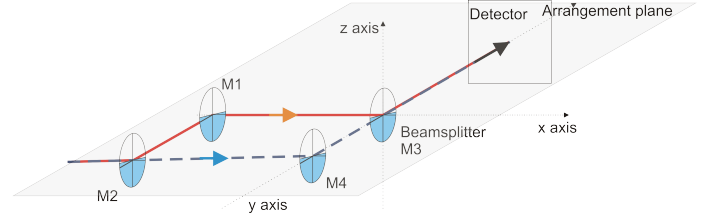


FIG. 5. Common Mach-Zehnder interferometer. The interferometer is a 2D interferometer.

\vec{k}_1 and \vec{k}_2 , respectively. If the incoming beam is not a central beam the propagated plane waves have a non vanishing wave vector component in the detector plane, the latter being perpendicular to the central beam. The k-vector projections on this plane are denoted by capital \vec{K}_1 and \vec{K}_2 , respectively. The interferometer of Figure 1 has the property

$$\vec{K}_1 = -\vec{K}_2 \quad (1)$$

We will further analyze the field transport in the generic interferometer of Figure 1. Two field directions are consecutively attached to the central beam which are transported by branch 1 and 2 (Figures 2, 3). The result by one branch (1 or 2) is always contrary or opposite to the other one. This is just the property of Equation (1) called 'k-flip'.

As can be expected from the introduction, this property is a result of a 3D field transport. Wavefront division can be excluded as a cause as shown by Figure 4. The figure shows that the incoming wave is split into two waves whereof one is displaced by a shift. The two newly introduced mirrors are parallel and do not introduce any rotation. As a result, the new set up is an interferometer with amplitude splitting which has the 'k-flip' property.

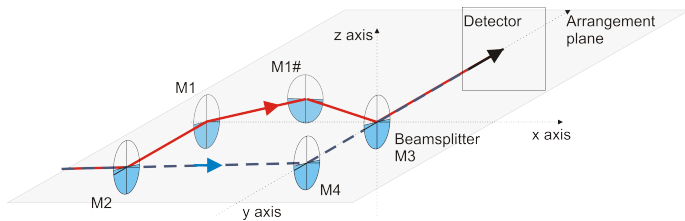


FIG. 6. The interferometer of Figure 5 with one additional mirror inserted into branch 2. The interferometer is a 2D interferometer.

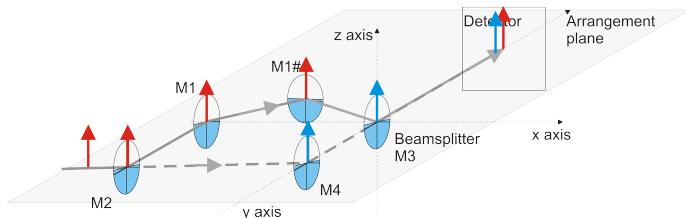


FIG. 7. Parallel transport in the interferometer as shown in Figure 6. The initial field direction is perpendicular to the arrangement plane. It can be seen that the parallel transport of the field direction does not lead to an inversion between the two branches.

2D interferometers do not have this property. Figure 5 shows a common 2D interferometer with two branches (a Mach-Zehnder interferometer). Figure 6 shows the same type of interferometer but with an additional mirror in one of the branches. In fact, this is the only design freedom we have in 2 dimensions.

It can be immediately seen that the Mach-Zehnder interferometer does not have the 'k-flip' property. Insertion of an additional mirror introduces an inversion of the field components in the arrangement plane, indeed (Figure 8). Yet orthogonal to this plane the situation remains unchanged (Figure 7). In conclusion, Equation (1) does not hold for both directions.

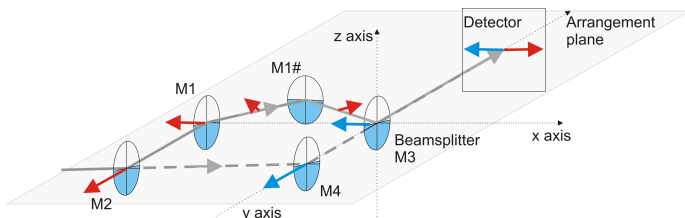


FIG. 8. Parallel transport in the interferometer as shown in Figure 6. The initial field direction is in the arrangement plane. It can be seen that the parallel transport of the field direction leads to an inversion between the two branches.

IV. EVALUATION FOR INCOHERENT SOURCES

We study the interferogram for an object consisting of incoherent emitters (sources) further. In addition, we assume that both branches have the same transmission. Thus, both plane waves have the same intensity. As we assume stationary, quasi-monochromatic light [2], each object point s leads to two beams which form an interference pattern with a real-valued, modulated intensity \mathcal{I} given by

$$\mathcal{I}_s(\vec{x}) = a_s * \cos(2K\vec{1}_s \cdot \vec{x} + \beta_s) \quad (2)$$

We have suppressed the constant term in Equation (2). \vec{x} is a 2D coordinate vector in the detector plane, β_s is a phase angle and a_s is a real-valued intensity parameter. The index s recalls the fact that the light comes from a source point called 's'.

Assuming a set of mutually incoherent sources this yields [2]

$$\mathcal{I}(\vec{x}) = \sum_s I(s) \mathcal{I}_s(\vec{x}) \quad (3)$$

$I(s)$ is the real-valued intensity of the light source s as introduced by [2]. This expression has to be well distinguished from the van Cittert-Zernicke theorem and the complex visibility $j(P_1, P_2)$ using the notation of M. Born and E. Wolf [2]. P_1 and P_2 denote the location of the two apertures in a 'division of wavefront' setup. In Figure 1 this is the location of the mirrors M1 and M2 having the coordinates P_1 and P_2 , respectively. $j(P_1, P_2)$ is measured by testing the 2-point coherence property at P_1 and P_2 . In principle, this can be done by any coherence sensitive experiment which compares light from P_1 and P_2 . It is the simplest approach to overlap the light coming from P_1 and P_2 and to look for any constructive or destructive interferences. Any visible interference pattern can be attributed to the mutual coherence properties of the light from P_1 and P_2 . Concerning this, it is unimportant how this interference pattern is actually produced. The Michelson stellar interferometer is a famous example [2]. Alternatively, two different telescopes can be used for P_1 and P_2 , thereby increasing the light sensitivity. Light wave variations over the experimentally finite areas of P_1 and P_2 are filtered out, similar to a fundamental mode filter. Although the finite extension of P_1 and P_2 is undesirable for the evaluation, a finite extension is needed to collect sufficient light. The light from P_1 and P_2 is brought to interference at an angle of incidence on the detector ($k \neq 0$). However, for all these cases, the k-vector of this interference is imposed by the setup and is independent of $K\vec{1}_s$. Furthermore, it should be emphasized that P_1 has nothing to do with \vec{x} in Equation (2).

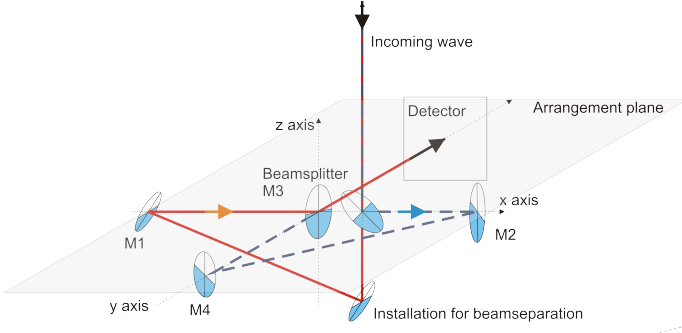


FIG. 9. The type of interferometer of Figure 4 but with some rearrangement of the branches such as to give the setup a more 'elegant' appearance. Furthermore, the two branches are symmetric and of similar or equal length.

It is the purpose of the Michelson stellar interferometer and its advanced multi-telescope successors to measure the size and location of stars. The complex degree of coherence $j(P_1, P_2)$ must be measured for many different pairs of P_1 and P_2 which together yield the image. This can be done by actively changing the setup (e.g. moving M1, M2) or by using either the earth or the satellite rotation. This method is called aperture synthesis.

In conclusion, the angular resolution obtained by aperture synthesis is not due to any particular 3D property of the interferometer but due to different measurements with different orientations of the whole interferometer in space.

The interference pattern recorded by an interferometer as shown in Figure 1 is very different from the previously described Michelson stellar interferometer since the former yields a real-valued intensity pattern described by Equation (3) whereas the latter produces a complex-valued 2-point correlation function $j(P_1, P_2)$. The former depends on the modulation of the light field over M1 and M2 while the latter does not measure this type of property.

To exemplify this further, we assume equal transmission for all 's' modes ($a_s = 1$). We call $I(s)$ the emission intensity of source point s . Equation (3) can then be reformulated

$$\mathcal{I}(\vec{x}) = \sum_s I(s) * \cos(2\vec{K}\vec{1}_s \cdot \vec{x} + \beta_s) \quad (4)$$

$K\vec{1}_s$ and β_s can be calculated, independently of the object, for every light point s , provided the interferometer is known. Alternatively the interferometer can be calibrated. If $\beta_s = \beta$ for all s , i.e. if β_s is independent of the index s , the point $x = 0$ is a point of stationary phase. The Equation (4) is a linear equation for $I(s)$. It is of course interesting to invert this equation to get $I(s)$ from measured results $\mathcal{I}(\vec{x})$. The solution is unique under certain conditions. If that is not the case, different measurement sets can be evaluated together, the diffraction

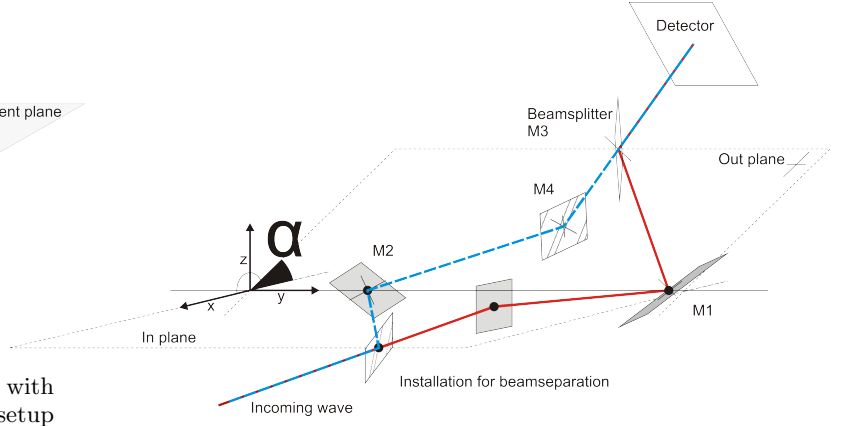


FIG. 10. A general field rotation. The twisting in 3 dimensions leads to a mutual field rotation between the light fields propagated by branch 1 and 2.

limit being a strict criterion for uniqueness.

The evaluation has many similarities with Fourier transform spectroscopy. The time or frequency variable in Fourier transform spectroscopy corresponds to the space or $\vec{K}\vec{1}$ vector variable in our concept. An application of the Wiener-Khinchine theorem [2] yields that the Fourier transform of the observed interference pattern $\mathcal{I}(\vec{x})$ corresponds to the real-valued spectral power density $I(\vec{K}\vec{1}_s) := I(s)$. Here, we denote the light source s by its wave vector component $\vec{K}\vec{1}_s$. This has some ambiguity since it is not possible to distinguish $\vec{K}\vec{1}$ from $-\vec{K}\vec{1}$ which can be seen from Equation (2) since $\vec{K}\vec{1}$ and $-\vec{K}\vec{1}$ yield the same pattern. The problem does not exist in the time domain, i.e. in classical Fourier transform spectroscopy as light always has a positive frequency [2]. However, the object in our setup usually consists of points to the 'right' and to the 'left' yielding both signs of $\vec{K}\vec{1}$. If this were not the case, the ambiguity would not arise. In fact, this has some similarity with a carrier phase method [1]. Alternatively, two data sets $\mathcal{I}(\vec{x})$ can be evaluated simultaneously with a slight sub wavelength change of path length in one of the branches. The fringe motion can be evaluated to distinguish between $\vec{K}\vec{1}$ and $-\vec{K}\vec{1}$.

In conclusion, this shows that an appropriate 3D interferometer yields valuable information about light emitting, incoherent objects. In the coherent case, mutual interference between different points 's' entails a different approach [4] (Section V).

V. EVALUATION FOR COHERENT WAVES

In the case of spatially coherent light, the incident wave has a well defined complex field $E(P)$ and the field values

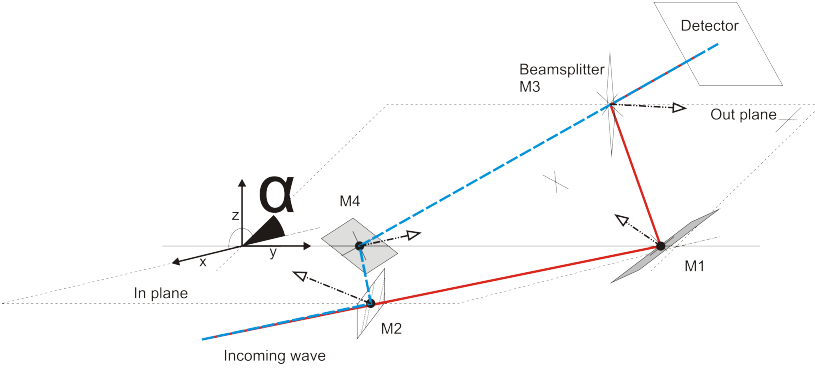


FIG. 11. A 3D interferometer with 4 beam reflections. In contrast to Figure 10 such an interferometer does not lead to a mutual field rotation.

at different points P are not only correlated but in a strict phase relation. In the case of amplitude splitting (Figures 4, 9) mutual phase relations can be measured in the detector plane. As a consequence, the complex field $E(P)$ can be determined.

In the most general case, two copies of the field called $E1$, $E2$ come to interference in the detector, $E1$ and $E2$ being the fields propagated by branch 1 and 2, respectively. In the following, it will be assumed that $E1$, $E2$ are the field functions defined in the plane of the detector. For an appropriate interferometer, $E2$ is determined by $E1$. The mapping can be determined by performing a back propagation of field $E1$ by branch 1 to a plane before the interferometer and a subsequent forward propagation by branch 2 to get $E2$. Thus, the mapping between $E1$ and $E2$ can include field propagation and diffraction effects which can be calculated exactly by solving Maxwell's equations (or e.g. the Helmholtz equation) [2]. This yields

$$E2_s = \sum_t U_{s,t} E1_t =: U(E1) =: UE1 \quad (5)$$

In this equation we introduce s and t as indices for different points on the detector. U is a linear mapping between $E1$ and $E2$ which is a property of the interferometer and not of a particular field.

The complex field $E1$ is obtained by solving a linear equation if U is known and if the interference and the amplitude of $E1$ are known from prior knowledge [4][5].

It is interesting to note that the incoherent case yields the real-valued power density $S(K\vec{1}_s)$ whereas the coherent case yields the complex-valued field $E1$. These types of interferometers are completely different.

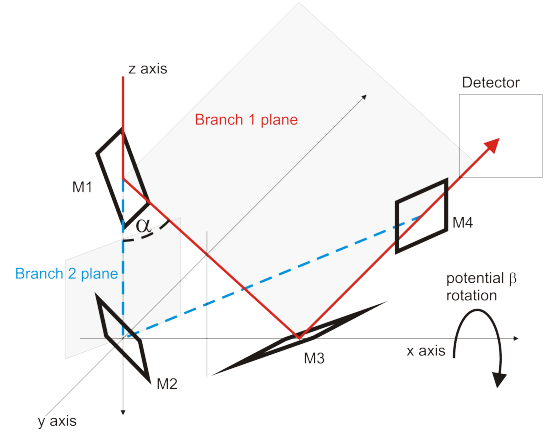


FIG. 12. The same type of interferometer as shown in Figure 11 but shown for a 90° folding of the interferometer planes. A plane 1 and 2 are depicted for branch 1 and 2, respectively. This makes it easier to track the field directions. This is done in Figure 13 and 14.

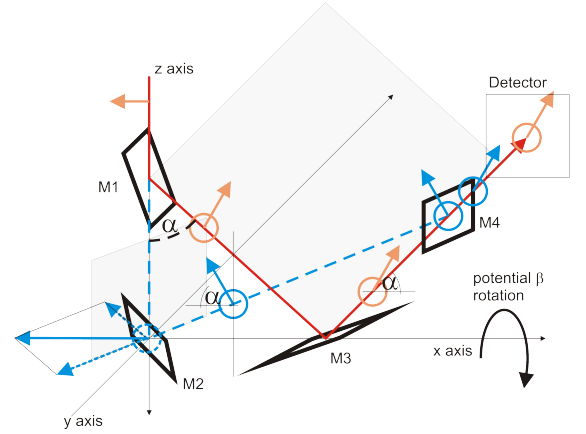


FIG. 13. The interferometer of Figure 12 with a depicted field direction. The parallel transport of this field direction is equal for branch 1 and 2. Thus, this type of equal path interferometer with 4 mirrors does not lead to a mutual field rotation.

VI. GENERAL 3D INTERFEROMETER

The mapping in Equation (1) corresponds to a 180° rotation called 'k-flip'. In the coherent case we introduced a mapping U which is more general. In particular, U might represent rotations other than 180° . Parallel transport can generate such rotations as shown in Figure 10. The interferometer consists of six wave reflections. Two reflections are performed by beam splitters at the entrance and the exit of the interferometer, four reflections are exerted by mirrors. The interferometer is characterized by an in-plane and an out-plane. The in-plane is defined by the transmitted and reflected beam on the input beam splitter. Referring to the output beam splitter, an out-

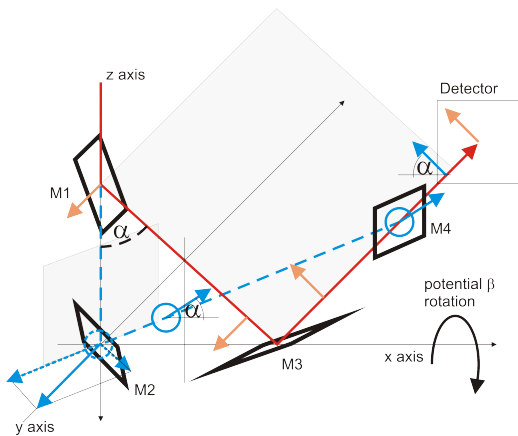


FIG. 14. The interferometer of Figure 12 with a depicted field direction orthogonal to Figure 13. The parallel transport of this field direction is equal for both branches (1 and 2). Thus, this type of equal path interferometer with 4 mirrors does not lead to a mutual field rotation.

plane can similarly be defined. The two planes form an angle α . Hence, they are not identical. If α becomes 90° the interferometer in Figure 10 is transformed into an interferometer as displayed in Figure 4, being actually a generalization of the latter.

For $\alpha = 0$ the field rotation in U becomes zero, for $\alpha = 90^\circ$ the field rotation in U is 180° . For all angles in between, smaller field rotations are generated. The mapping U is a rotation which entails the existence of a unique fixed point. This property is called the 'U-property' and replaces the 'k-flip' property known from the incoherent case in the coherent case.

It is interesting to note that the same cannot be achieved for an equal path interferometer with just four reflections as shown in Figure 11. The set of possible interferometer configurations is described by an ellipsoid with the two beam splitters at the foci. We analyze the four reflection setup in Figure 12 using an interferometer which is folded by an angle of $\beta = 90^\circ$. Holding β fixed the angle α can be varied. Figures 13 and 14 show that parallel transport does not lead to a mutual field rotation. It can be anticipated that this remains true for $\beta < 90^\circ$. For $\beta = 0^\circ$ we have a flat Mach-Zehnder interferometer. Of course such an interferometer does not possess a field rotation. In addition to that, we have verified by a numerical simulation that the field rotation is really zero for all intermediate β values. This actually proves the initial statement that a four reflection, equal path interferometer does not possess a field rotation.

This might be condensed into the statement that non-trivial, parallel transport only exists for a twisted interferometer with more than four mirrors whereas a folded interferometer with four reflections does not possess a mutual field rotation.

VII. CONCLUDING REMARKS

We have shown that an appropriate 3D interferometer possesses a mutual field rotation as observed in an interference between the field of branch 1 and 2. Thereby, a 3D interferometer is defined by one of the following definitions:

- An interferometer has the 3D property if the central beams do not lie in a plane, not even approximately (Type I).
- An amplitude division interferometer has the 3D property if the entrance plane given by the central beam at the first beamsplitter and the outgoing plane given by the central beams at the second beamsplitter are different (Type II).

The two definitions of 3D are essentially equal but the Type II property cannot be used for a wavefront division interferometer such as displayed in Figure 1.

The rotation properties can be expressed as a property of plane waves which are propagated differently by branch 1 and 2. The projection of the wave vectors on the detector plane denoted \vec{K}_1 and \vec{K}_2 have the 'k-flip' property

$$\vec{K}_1 = -\vec{K}_2 \quad (6)$$

For coherent light, the complex light fields are defined, E_1 and E_2 being the fields from branch 1 and 2, respectively. Therefore, a mapping U can be determined which describes the transformation in the interferometer, in particular the mapping from field E_1 to field E_2 .

$$E_2 = U(E_1) \quad (7)$$

If U has just one fixed point, the interferometer is said to have the 'U-property'.

If the light sources consist of incoherent emitters no field E_1 is defined and consequently no light field phase can be determined. The evaluation is based on an application of the Wiener-Khintchine theorem [2] which yields the real-valued power spectrum $S(K_1^2)$ of the K_1^2 distribution in the radiation field. Hence, an interferometer with the 'k-flip' property is needed.

On the other hand, coherent fields can be analyzed by an interferometer with the 'U-property'. The evaluation of the generated interferograms has become feasible due to the recent discovery of linear phase retrieval in SRI interferometers [4].

As a consequence, depending on the radiation field (coherent, incoherent) a different physical interferometer and a different evaluation method has to be used.

For this, the two properties ('k-flip' or 'U-property') are very useful and can be generated by an appropriately designed, twisted interferometer using parallel field transport.

-
- [1] T. Yoshizawa Editor, *Handbook of optical metrology*, 2nd ed. (CRC Press, Boca Raton, 2015)
 - [2] M. Born and E. Wolf, *Principles of optics*, 6th ed. (Pergamon Press, Oxford, 1991)
 - [3] Daniel Malacara editor, *Optical Shop Testing 3rd Edition*, John Wiley & Sons, 2007.
 - [4] Martin Berz, Cordelia Berz, *Unbiased (reference-free) phase field imaging for general optical fields including phase discontinuities*, arXiv 2016, arXiv:1610.08089, <https://arxiv.org/abs/1610.08089>
 - [5] Martin Berz, Cordelia Berz, *A new non-iterative self-referencing interferometer in optical phase imaging and holographic microscopy, HOLOCAM*, arXiv 2016, arXiv:1611.05765, <https://arxiv.org/abs/1611.05765>